

Flow Generation in a Narrow Space Using Dielectric Barrier Discharge

Keiichiro Yoshida¹, Ryusuke Sakamoto¹

¹Dept. of Electrical and Electronic Systems Engineering

Osaka Institute of Technology

phone: (81) 6-6954-4236

e-mail: keiichiro.yoshida@oit.ac.jp

Abstract—Ionic wind generation in the narrow space formed by two solid surfaces was investigated. In this study, dielectric barrier discharge (DBD) was used to generate ionic wind. The electrode was composed of 0.9 mm-thick dielectric plate made by glass, and a discharge electrode and a ground electrode made by aluminum tape. Narrow space was formed by two of such the electrodes facing to each other with distances between 0.5 and 1.8 mm. About 13.6 kHz ac high voltage with dc bias was applied to the discharge electrode. Results showed that when both the electrodes worked, flow of 1.0-1.2 m/s was generated in case where the gap between the electrodes was 0.5 mm.

I. INTRODUCTION

Applying high voltage to a pair of electrode in gas generates flow called ionic wind. It has been extensively studied in the fields of electrostatic precipitator [1], flow control on airfoils, enhancement of convection heat transfer, etc. Corona discharge and dielectric barrier discharge (DBD) are usually used for this purpose. [2–6]

One of the ultimate purposes of this study is an improvement of fin-tube heat exchanger performances. Heat exchanger with fins is used in a lot of types of thermal components, including heat radiators for engines in automobiles and heat-pumps such as air-conditioner, hot-water supply system, etc. If we could put a wind-generating function on fin surfaces, heat transfer coefficient is expected to be improved through reducing the temperature boundary layer. In this study, generating air flow produced by accelerated ions generated in DBD in a narrow space was investigated. This report shows basic characteristics of DBD electrodes with biases [2, 4–6] and its flow generation in the space formed by a pair of DBD electrodes.

II. EXPERIMENTAL APPARATUS

Figure 1 (a) and (b) show the electrodes investigated in this study. Pyrex glass of 0.9 mm thickness was used for the dielectric layers.

The electrode shown by Fig. 1 (a) (type A) are composed of a discharge electrode and a collector electrode on the upper surface, and a ground electrode on the bottom surface. The ground electrode is sealed with epoxy resin to avoid discharge on the bottom surface.

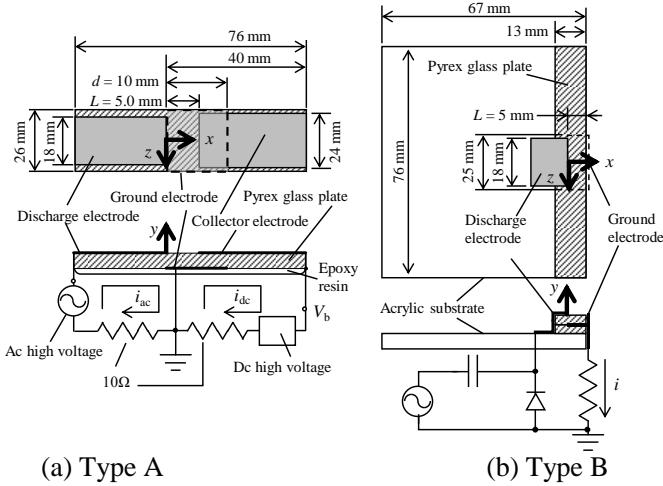


Fig. 1. Schematics of DBD electrodes for flow generation.

Ac high voltage is applied between the discharge and ground electrodes. Dc high voltage is applied to the collector electrode. The current i_{ac} and i_{dc} , which are defined in Fig. 1 (a) are measured separately using 10 ohm resistors. The positive direction of those currents are also defined in Fig. 1 (a). The width of the discharge, ground, and collector electrodes are 18, 26, and 24 mm, respectively. The ground electrode is 10 mm long. The collector electrode faces to the discharge electrode with the gap of 5 mm. xyz -axes are defined as shown in Fig. 1 (a). The origin is placed at the center of the discharge-electrode edge. z -axis goes along the edge of the discharge electrode. y -axis is perpendicular to the surface of the glass plate. The edges of the discharge electrode and the ground electrode coincide in x -coordinate.

Fig. 1 (b) shows the type B electrode. Its ground electrode also plays the role of a collector electrode. This structure can simplify the electric circuit for the type A electrode. The discharge electrode is provided with ac high voltage superimposed with dc voltage by using a rectifying circuit. xyz -axis is also defined as is in type A. A Pyrex glass plate of 76 mm width and 13 mm length is used as a dielectric layer. A discharge electrode of 18 mm width and a ground electrode of 24 mm width are attached to the upper and bottom surface, respectively. The edge of the discharge electrode is placed at the position of 5 mm from the edge of the glass plate. One edge of the ground electrode coincides with the discharge-electrode edge in x -coordinate and the other edge reaches the upper-surface edge of the glass plate. The current i is measured using a 10-ohm resistor.

Figure 2 shows an experimental setup for measuring flow velocities. A glass capillary tube of 1.0 mm outer diameter and 0.6 mm inner diameter is placed facing the flow. The position of the capillary is adjusted with a micromotion stage. The total pressure at the tip of the capillary is measured with an electronic balance with a cylinder half soaked in silicone oil. The inner diameter of the cylinder is 30 mm. Flow velocity v is calculated from the difference between the total and static pressure, which is also measured by the electronic balance.

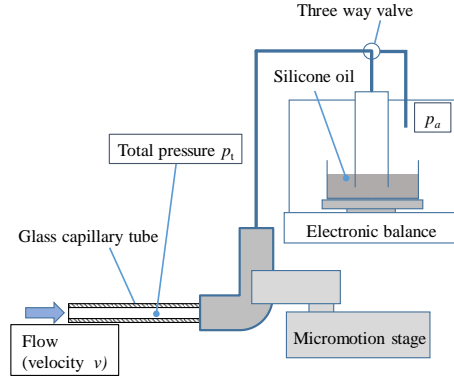


Fig. 2. Measurement system for flow velocity

III. RESULTS AND DISCUSSION

The results for type A will be explained first. Typical wave forms of applied voltage, current i_{ac} and i_{dc} are shown in Fig. 3. These waves were obtained by applying ac voltage of 13.6 kHz and V_{pp} (peak-to-peak voltage) of 6.16 kV and dc voltage (V_b) of -2.25 kV. The applied ac voltage is not a sinusoidal wave but a wave with sharp positive peaks. The voltage changing rate is particularly large when it goes from negative to positive. Large pulsed of i_{ac} and i_{dc} arise intensively right before the voltage positive peak. Both the current peaks are positive. The reason that i_{ac} and i_{dc} have oscillatory peaks is not clear at this stage. The occurrence of i_{dc} indicates that charged particles move toward the collector electrode.

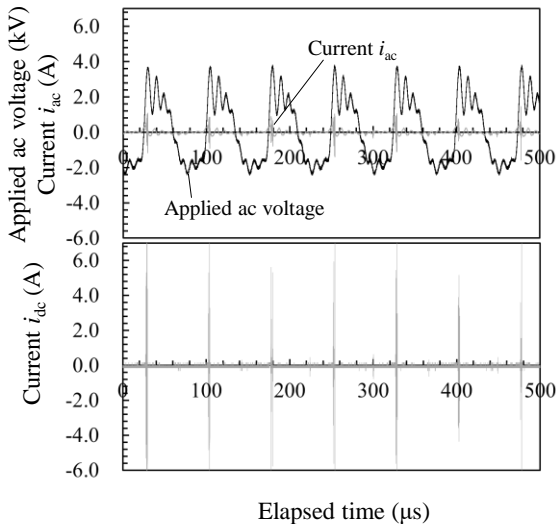


Fig. 3. Typical waveforms of applied voltage and currents for type A electrode ($f = 13.6$ kHz, $V_{pp} = 6.06$ kV, $V_b = -2.25$ kV).

Figure 4 shows the relationship between flow velocities v , and peak-to-peak voltage V_{pp} of applied voltage and bias voltage V_b . The coordinates x , y , and z of the position where the velocities were measured is 5, 0.5, and 0 mm, respectively. The flow in x direction did not occur below 4 kV_{pp}. v increases with increasing V_{pp} with the maximum velocity of 1.5 m/s at V_{pp} of 5.75 kV and V_b of -3.0 kV. In case where no bias voltage was applied, as small as approximately 0.22 m/s of flow was obtained. The effect of applying the bias voltage could be seen only for $V_b < 0$. This fact indicates that mainly positive ions contribute to generate air flow. The result that significant breakdown of air only arose at the moment of around the positive peak supports this idea as can be seen in Fig. 3. To compare velocities v with different V_b at the same V_{pp} , v increased rapidly with the decrease in V_b down to -2.25 kV and increased more slowly with V_b lower than -2.25 kV.

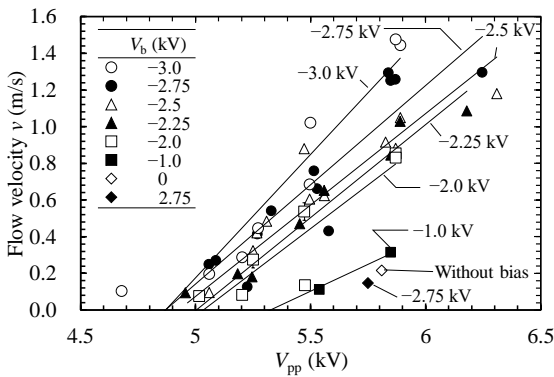


Fig. 4. Flow velocities in x -direction for type A electrode.

Figure 5 shows the P_t , which is the sum of the consumed powers in the dc-bias and the ac circuits, as a function of V_{pp} with different V_b s. The consumed power in each the circuit was separately obtained by time-integrating the product of current and applied voltage. Larger P_t can be seen with lower V_b . It was observed that i_{ac} also increased with decreasing V_b (not shown in this report though). The collector electrode applied with negative voltage might have absorb positive ions, causing higher electric field at the vicinity of the discharge electrode when ac applied voltage came to positive peaks.

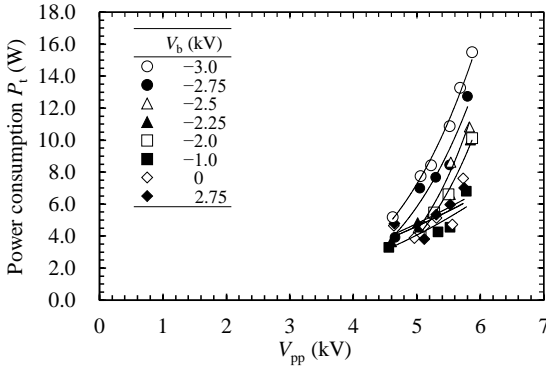


Fig. 5. The power consumptions at type A electrodes Pt as functions of peak-to-peak voltage of applied ac voltage V_{pp} with different dc bias voltages V_b .

The results of type B electrode will be explained. Figure 6 shows the voltage applied to the discharge electrode and the current i . The rectifying circuit described in Fig. 1 (b) shifts the ac voltage in positive direction, realizing the same effect as applying type A electrode with negative V_b . Dc voltage (= mean applied voltage V_{mean}) of 2.3 kV is superimposed to ac voltage when peak-to peak voltage is 6 kV_{pp}. Positive current pulses arise right before the positive peaks of the applied voltage. The reason for the oscillation of current peaks is not clear at this stage. The current i in type B electrode is almost the same as the sum of i_{ac} and i_{dc} observed in type A electrode. Positive ions drift at this moment of current pulses.

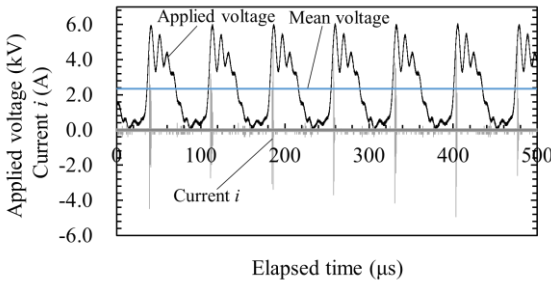


Fig. 6. Typical waveform of applied voltage and current for type B electrode ($f = 13.6$ kHz, $V_{pp} = 6.06$ kV, and $V_{mean} = 2.34$ kV).

Figure 7 shows flow velocities in x -direction v with respect to the distance from the surface y . The peak-to-peak and the mean of the applied voltage were approximately 6 kV and 2.3 kV, respectively for the cases in this figure. The consumed power is 16–18 W, which corresponds to the results in type B electrode provided with the equivalent V_{pp} and V_b . Velocities of 0.8–1.3 m/s were observed at y of 0.25 and 0.5 mm. The velocities decreased with increasing y . When y is 1.5 mm, the velocities were roughly 1/3 of the values at y of 0.25 and 0.5 mm.

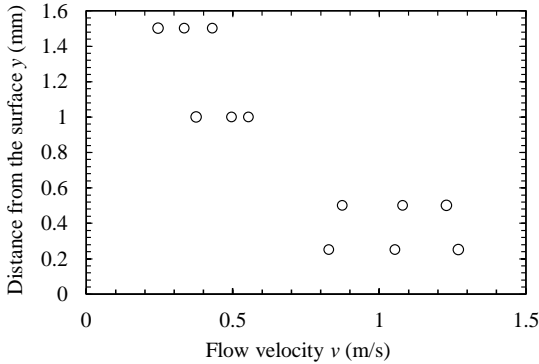


Fig. 7. Flow velocity distribution over the surface of type B electrode ($f = 13.6$ kHz, $V_{pp} = 6$ kV, and $V_{mean} = 2.3$ kV).

Two of type B electrodes were placed facing each other illustrated in Fig. 8. The distance between the surfaces of the glass plates is defined as h .

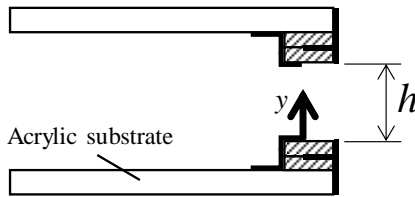


Fig. 8. Schematics of the narrow space formed by two of type B electrodes.

Figure 9 shows the velocity distributions in cases where the distance $h = 1.8, 0.9,$ and 0.5 mm. The flow velocities in x -direction were measured at $z = 0$ and $x = 5$ mm (at the exit of the narrow spaces). Two kinds of results are shown— upper and lower electrodes were operated (circular symbol), and only lower electrode was operated (triangular symbol). In case where only lower electrode was operated, the velocity distribution of $h = 1.8$ mm is almost the same as that of the open-space experiment shown in Fig. 7. For smaller h , larger velocity gradient made the velocities smaller. In cases where both the electrodes were operated, the decrease in velocities with decreasing h was less severe. Even at h of 0.5 mm, $1\text{--}1.2$ m/s was obtained. In addition, lower velocities at higher y even in the case where both the electrodes were operated were caused by the individual differences in type B electrodes.

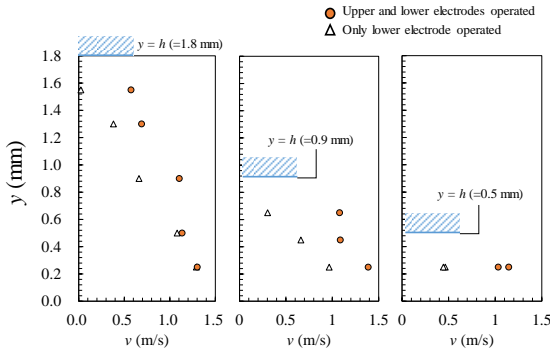


Fig. 9. Flow distribution in the space formed by two of type B electrodes.

IV. CONCLUSION

In this work, the basic characteristics of DBD electrodes for flow generation in air were investigated. Ac high voltage with dc bias voltage was applied to the discharge electrodes and the flow velocities were shown for different applied voltages. Probably because of positive sharp peaks of applied ac voltage, ionic wind was generated more efficiently in case where the applied voltage to the discharge electrode has a positive dc component with respect to the collector electrode. Flow velocities between the narrow space (the gap between them ranged from 0.5 to 1.8 mm) formed by a pair of DBD electrodes were measured and velocities of 1.0–1.2 m/s were found for the pair that has 0.5 mm gap.

REFERENCES

- [1] H. Fujishima, Y. Ueda, K. Tomimatsu, T. Yamamoto, "Electrohydrodynamics of spiked electrode electrostatic precipitators", *J. Electrostat.*, vol. 62, pp. 291–308, 2004.
- [2] J Jolibois, K Takashima and A Mizuno, "Effects of a transmission line on the properties of a surface discharge based on a segmented ground electrode design", *J. Appl. Phys.: Conference Series*, vo. 301, 012021, 2011.
- [3] C. Kim, D. Park, K. C. Noh, and J. Hwang, "Velocity and energy conversion efficiency characteristics of ionic wind generator in a multistage configuration", *J. Electrostat.*, vol. 68, pp. 36–41, 2010.
- [4] E. Moreau, R. Sosa, and G. Artana, "Electric wind produced by surface plasma actuators: a new dielectric barrier discharge based on a three-electrode geometry", *J. Appl. Phys. D*, vol. 41, 115204 (12pp), 2008.
- [5] E. Moreau, C. Louste, and G. Touchard, "Electric Wind induced by sliding discharge in air at atmospheric pressure", *J. Electrostat.*, vol. 66, pp. 114–117, 2008.
- [6] E. Moreau, "Airflow control by non-thermal plasma actuator", *J. Phys. D*, vol. 40, pp. 605–636, 2007.